



Lasers in Manufacturing Conference 2019

Tailored femtosecond laser fabrication of reflective waveplates

A. San Blas^{1,2}, N. Casquero^{1,2}, M. Martínez-Calderón^{1,2}, J. Buencuerpo^{3*}, L.M. Sanchez-Brea³, J. del Hoyo³, S.M. Olaizola^{1,2}, A. Rodríguez^{1,2}, M. Gómez-Aranzadi^{1,2}

¹ Ceit, Manuel Lardizabal 15, 20018 Donostia / San Sebastián, Spain

² Universidad de Navarra, Tecnun, Manuel Lardizabal 13, 20018 Donostia / San Sebastián, Spain

³ Applied Optics Complutense Group, Optics Department, Universidad Complutense de Madrid, Facultad de Ciencias Físicas, Ciudad Universitaria s.n., 28040, Madrid, Spain

*Now in: National Renewable Energy Laboratory, Golden, Colorado (USA)

Corresponding author: yolaizola@ceit.es

Abstract

Laser induced periodic surface structures (LIPSS) can be studied as waveplates due to the birefringence induced by the nanoripples, with easy fabrication since they are fabricated in a one-step process by laser, where LIPSS geometry are defined by the characteristics of the laser and the substrate. The optical properties of these waveplates are defined by LIPSS parameters such as period, depth or width of the ripples. In this work we have measured the change in polarization of the light reflected from LIPSS generated on stainless steel. Results show a gradual change in polarization as the parameters employed in the fabrication vary. As shown in our experiments with a setup based in cylindrical focusing lens, the fast fabrication of samples with applications as waveplates is demonstrated.

Keywords: LIPSS; femtosecond; nanostructures; polarization; waveplate; laser

1. Introduction

Polarization control is a fundamental requisite in many experimental setups in optics and photonics. For this purpose, waveplates are used. Waveplates introduce a fixed phase delay between the orthogonal components of the electric field, which changes the polarization of the incident beam. Commonly used waveplates are transmissive, employing birefringent materials with varying thicknesses depending on the desired effect. However, some experiments require lower temporal dispersion or higher damage threshold. Since crystals may not be suitable for these cases, reflective waveplates based in periodic gratings fabricated with lithography or laser interference methods are readily available, although with drawbacks such as time-consuming fabrication, use of pollutants, or narrow range of grating periods available.

A well-known method for the production of nanostructures is laser technology. In 1965, Laser-Induced Periodic Surface Structures (LIPSS) were discovered. These structures, with period similar to the wavelength of the incident light, appear in most types of materials when irradiated with laser light, and their properties (such as periodicity or height) can be controlled with fluence, wavelength or pulse duration of the incident light. LIPSS have been widely used for surface functionalization with applications such as fabrication of hydrophilic/phobic surfaces (M. Martínez-Calderón et al., 2016), mechanical stress detection (S. Gräf et al., 2019) or colorization (B. Dusser et al., 2018). However, to the best of our knowledge, they have not been applied as gratings for reflective waveplates.

Here we report the fabrication of reflective waveplates using femtosecond laser technology. By focusing the laser beam with a cylindrical lens onto stainless steel samples, LIPSS are generated on their surface, making this a fast, one-step fabrication method. We show as well that by varying the parameters employed in the fabrication, the properties of the waveplate can be controlled.

2. Materials and methods

2.1. Laser setup

A Ti:Sapphire laser was used to irradiate the stainless steel samples in order to create LIPSS on its surface. The laser system produces 120 fs pulses with central wavelength of 800 nm and repetition rate of 1 kHz. The pulse energy was adjusted with a variable attenuator consisting of a half-wave plate and a polarizer. A motorized half-wave plate rotates the polarization of the laser beam. A combination of a cylindrical lens with focal 100 mm and a spherical lens with focal 75 mm is finally used to focus the beam on the sample with a line profile perpendicular to the X-axis. A CMOS camera using a white LED as illumination was used to monitor the process, as shown in Fig 1. XZ motorized stages were used to hold the sample and to control the projected line size and processing speed.

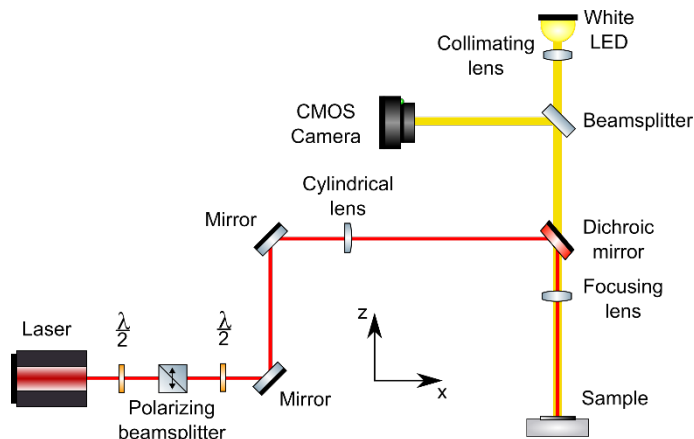


Fig. 1. Setup used in the processing of the samples

2.2. Fabrication process

The irradiated material was polished stainless steel in samples of dimensions 10 mm x 20 mm. Before and after the process the sample was introduced in acetone ultrasound bath in order to remove dirt and particles generated during the process.

The sample was moved under the laser beam at a constant speed along the X-axis. The position in the Z-axis was adjusted so that the width of the laser beam projected onto the sample was 30 μm . The range of speeds used for the different samples was between 0.8 and 2.4 mm/s. The energy used for all the samples was 1.4 mJ. The polarization of the laser light was parallel to the motion of the X-axis.

2.3. Characterization

The effect of the fabricated samples on the incident light was measured with a polarimeter (Thorlabs PAX1000IR1). A He-Ne laser (633 nm wavelength) was incident at 5° with respect to the normal of the sample. Incident laser polarization was controlled with a half wave plate. To better detect birefringence, incident polarization was set to linear at 45° with respect to LIPSS orientation. The specular reflection of light was analyzed with the polarimeter.

The changes in the surface of the samples were characterized with SEM (Scanning Electron Microscope), and 2D-FFT (two-dimensional Fast Fourier Transform) was applied to the images taken to measure the periodicity of the generated LIPSS, since the relation between LIPSS period (Λ) and the distance between FFT peaks (d) is given by the equation $\Lambda=2/d$. Height measurements were obtained with AFM (Atomic Force Microscope) sweeps that were performed in large areas of 30 μm x 30 μm . Vertical distance between positive and negative peaks were measured and averaged to obtain the average height of the sample. Images of the transversal profile of LIPSS were obtained through the FIB (Focused Ion Beam) technique implemented in a SEM microscope.

3. Results and discussion

Results obtained from the polarimeter show that the ellipticity of the beam polarization can be modified by varying the processing speed. As processing speed increases from 0.8 mm/s to 1.6 mm/s, ellipticity also increases from 2.91° to 11.04°. However, as the speed further increases, the ellipticity starts to decrease again to 1.18° at a speed of 2.4 mm/s. Therefore, a change in the polarization is observed, from linear to elliptical, with a varying degree of ellipticity that changes smoothly with processing speed. At the same time, an effect on the reflectivity is seen. It increases continuously from 2.2% at 0.8 mm/s to 13% at 2.4 mm/s. Reflectivity of a stainless steel sample is 38%.

The coherence in the results between samples suggest that the setup used in the fabrication allows a consistent fabrication where the parameters are kept constant, especially laser spot size. Unlike other processing setups that use microscope objectives with working distances of a few millimeters, our setup uses long focal lenses and therefore has long Rayleigh length, which helps in the positioning of the sample in the Z axis. Also, the cylindrical lenses used in this experiment allow a simpler processing strategy. Since the projected line on the sample is long enough to cover one of the axes, the samples only need to be translated along the axis perpendicular to the laser line. The required time for the processing of the sample is therefore greatly reduced.

A study of the LIPSS morphology has been carried out. Fig 2 shows a comparison between the surface of two samples, corresponding to processing speeds of 0.8 mm/s (left) and 1.6 mm/s (right). These samples are of interest because they represent the lowest (0.8 mm/s) and highest (1.6 mm/s) change in polarization observed. A slight difference in the shape of the LIPSS can be seen in the left image, where the ripples show imperfections along the crest. This effect has been reported in literature, which is caused by the lower processing speed and higher total fluence. On the other hand, the right image shows LIPSS that are better

defined without as many imperfections. The 2D-FFT images show two main peaks in intensity to each side of the origin (in the center of the image). It can be seen that our LIPSS are not perfect structures, since there is not a single point corresponding to a single frequency and orientation. Instead, there is a stronger peak and a weaker one at double frequency, both with some range of frequencies and orientations that vary between samples. These imperfections could be one of the effects limiting the effectiveness of the resulting grating, reducing the reflectivity and ellipticity change.

Measuring from the obtained 2D-FFT images the distance from the point of maximum intensity to the origin gives the main frequency or period of the LIPSS. The period of the generated LIPSS increase linearly with the processing speed, from 602 to 651 nm. We expect the period of the LIPSS to be a key factor in the behavior of the grating.

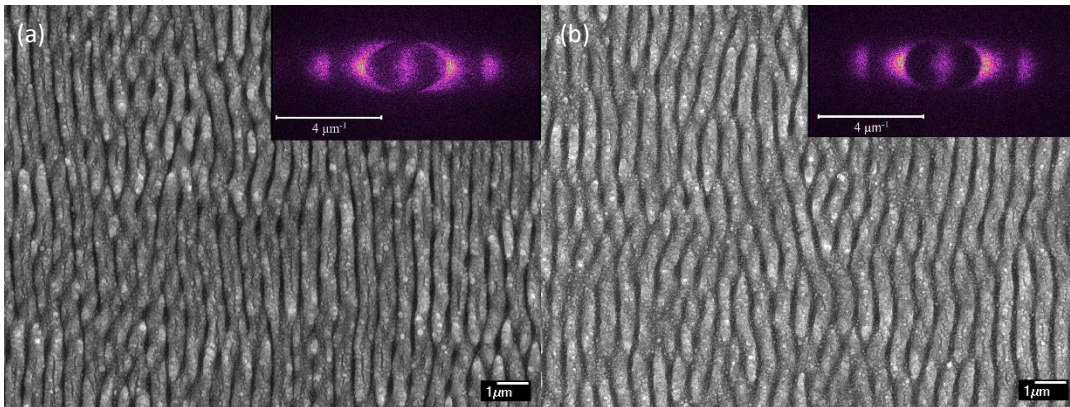


Fig. 2: SEM images of samples fabricated at a) 0.8 mm/s and b) 1.6 mm/s. Insets: 2D-FFT of the samples.

Results found from the AFM measurements show that height is similar between the studied samples. Therefore, we confirm that height is not a factor in the reflective behavior of our samples. Fig 3 shows an example of FIB profile, where the LIPSS irregularity exemplifies the difficulty of obtaining a single value for the height. Also, similar structures and heights are observed between the two methods (AFM and FIB), concluding that both are a valid source of data.

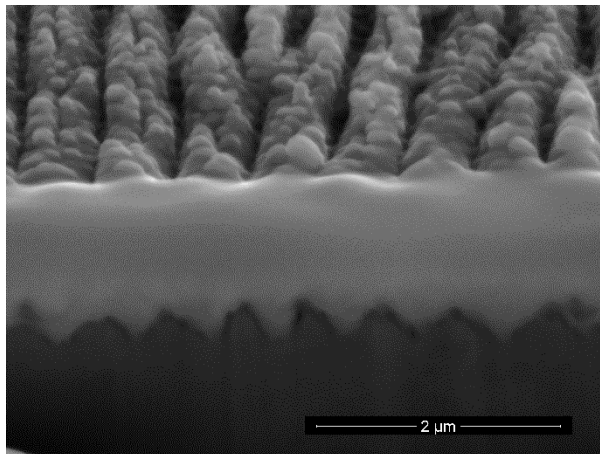


Fig. 3: FIB section of a sample processed at 0.8 mm/s. Structures with different profiles can be seen.

4. Conclusion

In this work, we have proven the fast fabrication of LIPSS on stainless steel samples with a setup based on cylindrical lens and their potential application as reflective waveplates. Sample fabrication can be performed at a speed in the order of 1 mm/s because of the use of cylindrical lens that also allows a stable and replicable fabrication, with little to no error between the consecutive samples fabrication

The maximum change in ellipticity achieved is 11°, although we expect higher values in future experiments. We have studied the morphology of LIPSS and, although the exact relation between polarization change and LIPSS morphology is yet not well understood due to the variety of factors in play (profile shape, period, or irregularities), two are the main factors that we have found could be affecting this change: periodicity and LIPSS regularity and homogeneity.

References

- M. Martínez-Calderón, A. Rodríguez, A. Dias-Ponte, M.C. Morant-Miñana, M. GómezAranzadi, S.M. Olaizola, 2016. "Femtosecond laser fabrication of highly hydrophobic stainless steel surface with hierarchical structures fabricated by combining ordered microstructures and LIPSS", *Appl. Surf. Sci.*, 374, 81–89.
- S. Gräf, C. Kunz, A. Undisz, R. Wonneberger, M. Rettenmayr, F. A. Müller, 2019. "Mechano-responsive colour change of laser-induced periodic surface structures", *Appl. Surf. Sci.*, 471, 645–651.
- B. Dusser, Z. Sagan, H. Soder, N. Faure, J.P. Colombier, M. Jourlin and E. Audouard, 2010. "Controlled nanostructures formation by ultra fast laser pulses for color marking", *Optics Express*, 18, 3, 2913–2924.